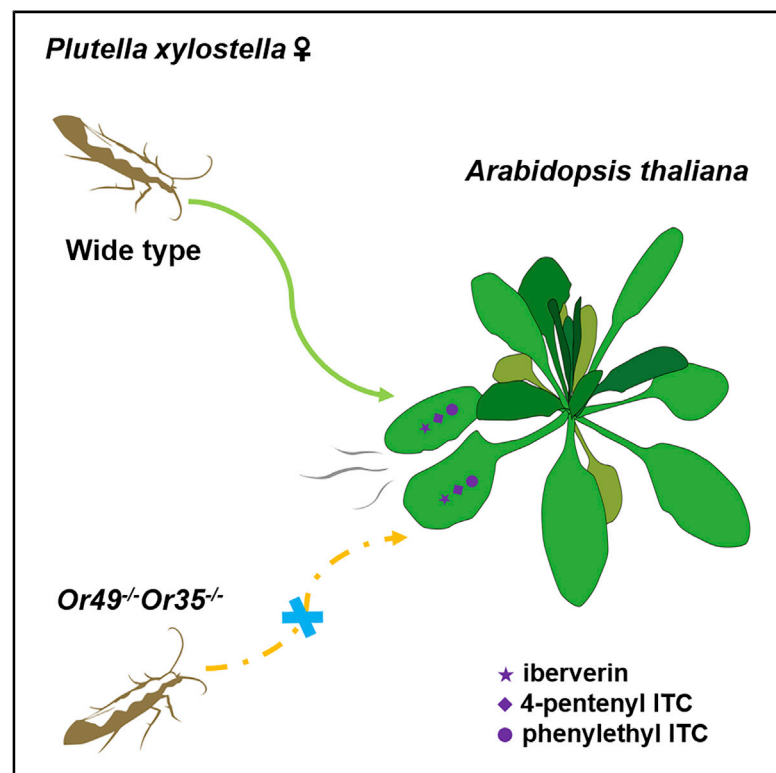


Current Biology

The Molecular Basis of Host Selection in a Crucifer-Specialized Moth

Graphical Abstract



Authors

Xiao-Long Liu, Jin Zhang, Qi Yan, ..., Chen-Zhu Wang, Shuang-Lin Dong, Markus Knaden

Correspondence

sldong@njau.edu.cn (S.-L.D.),
mknaden@ice.mpg.de (M.K.)

In Brief

Liu et al. provide evidence that Or35 and Or49 together are necessary and sufficient for detecting isothiocyanates and host plant in female *Plutella xylostella*. The results, for the first time, identify the molecular basis of host selection in a cruciferous specialist.

Highlights

- Isothiocyanates stimulate the oviposition of female *Plutella xylostella*
- Female-enhanced receptors Or35 and Or49 respond to isothiocyanates
- Or35 and Or49 together are necessary and sufficient for detecting isothiocyanates



Report

The Molecular Basis of Host Selection in a Crucifer-Specialized Moth

Xiao-Long Liu,^{1,4} Jin Zhang,^{2,4} Qi Yan,¹ Chun-Li Miao,¹ Wei-Kang Han,¹ Wen Hou,¹ Ke Yang,³ Bill S. Hansson,² Ying-Chuan Peng,¹ Jin-Meng Guo,¹ Hao Xu,¹ Chen-Zhu Wang,³ Shuang-Lin Dong,^{1,5,*} and Markus Knaden^{2,*}

¹Key Laboratory of Integrated Management of Crop Disease and Pests, Ministry of Education/ Department of Entomology, College of Plant Protection, Nanjing Agricultural University, 210095 Nanjing, China

²Department of Evolutionary Neuroethology, Max Planck Institute for Chemical Ecology, 07745 Jena, Germany

³State Key Laboratory of Integrated Management of Pest Insects and Rodents, Institute of Zoology, Chinese Academy of Sciences, 100101 Beijing, China

⁴These authors contributed equally

⁵Lead Contact

*Correspondence: sldong@njau.edu.cn (S.-L.D.), mknaden@ice.mpg.de (M.K.)

<https://doi.org/10.1016/j.cub.2020.08.047>

SUMMARY

Glucosinolates (GSs) are sulfur-containing secondary metabolites characteristic of cruciferous plants [1, 2]. Their breakdown products, isothiocyanates (ITCs), are released following tissue disruption by insect feeding or other mechanical damages [3, 4]. ITCs repel and are toxic to generalist herbivores, while specialist herbivores utilize the volatile ITCs as key signals for localizing host plants [5, 6]. However, the molecular mechanisms underlying detection of ITCs remain open. Here, we report that in the diamondback moth *Plutella xylostella*, a crucifer specialist, ITCs indeed drive the host preference for *Arabidopsis thaliana*, and the two olfactory receptors Or35 and Or49 are essential for this behavior. By performing gene expression analyses, we identified 12 (out of 59 in total) female-biased *Ors*, suggesting their possible involvement in oviposition choice. By ectopically expressing these *Ors* in *Xenopus* oocytes and screening their responses with 49 odors (including 13 ITCs, 25 general plant volatiles, and 11 sex pheromone components), we found that Or35 and Or49 responded specifically to three ITCs (iberverin, 4-pentenyl ITC, and phenylethyl ITC). The same ITCs also exhibited highest activity in electroantennogram recordings with female antennae and were the strongest oviposition stimulants. Knocking out either Or35 or Or49 via CRISPR-Cas9 resulted in a reduced oviposition preference for the ITCs, while double *Or* knockout females lost their ITC preference completely and were unable to choose between wild-type *A. thaliana* and a conspecific ITC knockout plant. We hence conclude that the ITC-based oviposition preference of the diamondback moth for its host *A. thaliana* is governed by the cooperation of two highly specific olfactory receptors.

RESULTS

Isothiocyanates Stimulate the Oviposition of Female *P. xylostella*

We first examined the egg-laying preference of female *P. xylostella* toward plant homogenate of *A. thaliana* and a panel of 13 ITCs using a two-choice assay in an oviposition cage (Figure 1A). While the homogenate turned out to be the most attractive cue (Figure 1B), all 13 representative ITCs tested significantly attracted the moths as compared to the solvent control. Notably, three ITCs (iberverin, 4-pentenyl ITC, and phenylethyl ITC, which is also present in the *A. thaliana* homogenate; Figure S1, bottom) were significantly preferred compared to the other odorants (Figure 1B). Interestingly, when performing electroantennogram recordings (EAGs), although the plant homogenate again yielded the strongest responses, the three ITCs that stimulated oviposition most significantly also elicited the strongest EAG responses among the individual compounds tested (Figure 1C).

Or35 and Or49 Are Tuned to ITC Compounds

To gain insights into the molecular mechanisms of ITC detection in female *P. xylostella*, we performed an expression analysis for all olfactory receptor genes. We assumed that the expression of *Ors* involved in the detection of the ITCs that govern oviposition behavior should be abundant in females (although it should be mentioned that a female-specific increase of the expression of a given *Or* does not necessarily mean that this receptor is involved in oviposition, as other female-specific behaviors like flower feeding, mate choice, etc. might be odor driven as well). A qRT-PCR with the 49 *Ors* known from *P. xylostella* (Figure S2) revealed that the expression of 12 *Ors* was female biased (Figure 2A).

We ectopically expressed all 12 *Ors* individually, but together with the insect odorant co-receptor *Orco* in *Xenopus* oocytes, and tested their responses to the aforementioned 13 ITC compounds (concentration, 10^{-4} M) by using a two-electrode voltage-clamp recording system. Ten of the 12 *Ors* did not respond to any of the ITCs (Figure S3). However, Or35/*Orco*



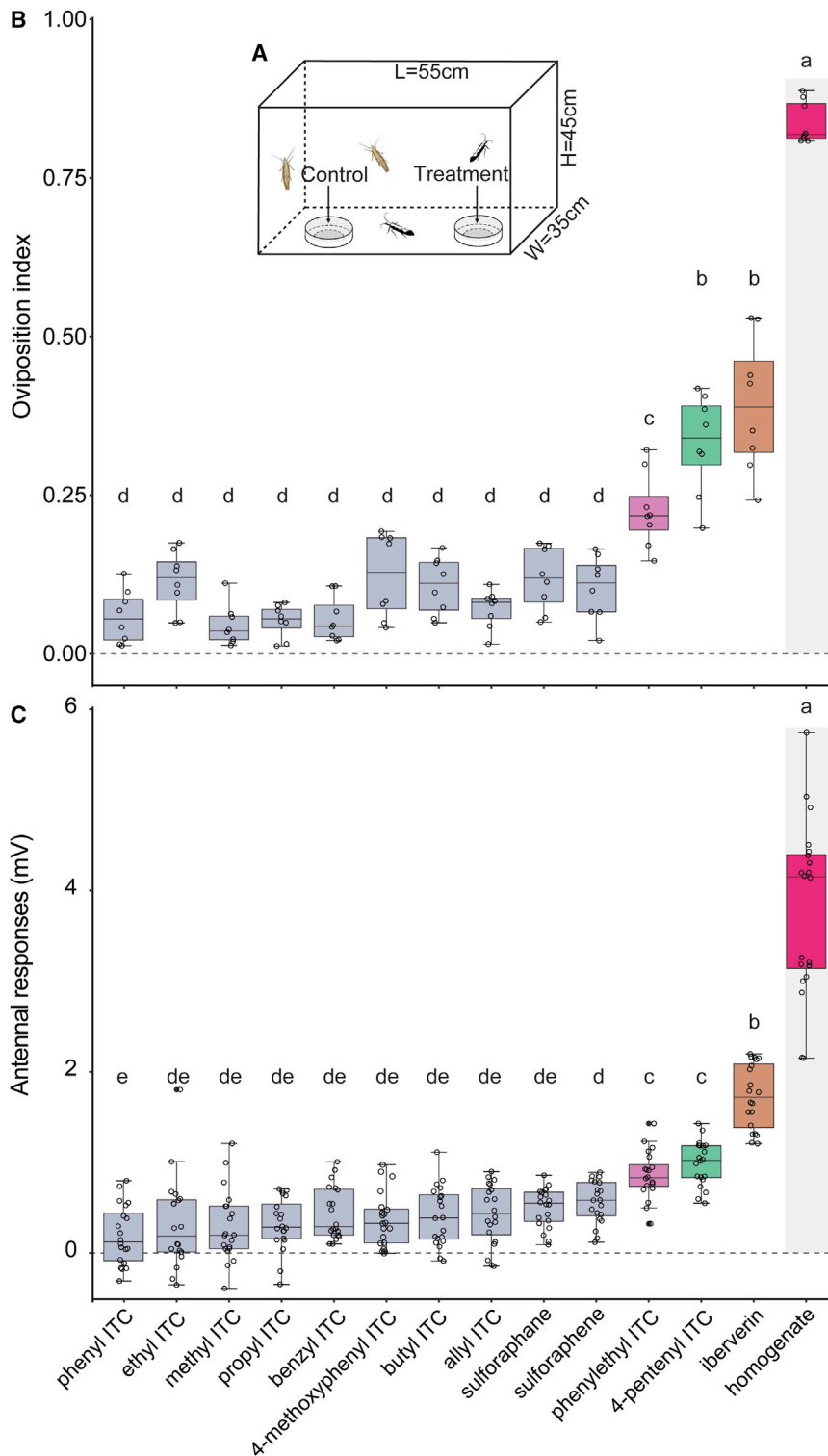


Figure 1. Isothiocyanates Stimulate the Oviposition of Female *P. xylostella*

(A) Schematic drawing of oviposition assays. (B) Oviposition index of females toward 13 ITCs and homogenate of *A. thaliana* leaf. Oviposition index = (number of eggs at treatment – number of eggs at control) / number of total eggs. Letters denote the significant differences among 13 ITCs and homogenate of *A. thaliana* leaf (one-way ANOVA followed by Tukey's pairwise test; $p < 0.05$). All attraction indices were significantly higher than zero. Deviation of the oviposition index against zero was tested with Wilcoxon signed-rank test ($n = 8$). (C) EAG responses (for each animal, the response to solvent was subtracted from the odorant response) of antenna isolated from WT females. Letters denote the significant differences among 13 ITCs and homogenate of *A. thaliana* leaf (one-way ANOVA followed by Tukey's pairwise test; $p < 0.05$) ($n = 20$). Boxplots depict median and upper and lower quartile; whiskers depict quartiles $\pm 1.5 \times$ the interquartile range (IQR). All data were included in the statistical analysis. See also [Figure S1](#) and [Table S3](#).

compounds, including 25 host plant volatiles and 11 female sex pheromone compounds and their analogs, did not result in any activation ([Figure S3](#)).

We therefore conclude that Or35 and Or49 are selectively tuned to the detection of the ITCs that govern oviposition.

Or35 and Or49 Together Are Necessary and Sufficient for Detecting ITC Compounds

To investigate the localization of Or35- and Or49-expressing cells in the antenna, two color *in situ* hybridization with antisense RNA probes for Or35 (red) and Or49 (green) were conducted on cryo-sections through antenna from wild-type (WT) female *P. xylostella*. As shown in [Figure 3A](#), Or35 and Or49 were co-localized in the same trichoid sensilla. Next, to address the contribution of Or35 and Or49 in the ITC-governed oviposition choice, we used CRISPR-Cas9 genome editing to generate Or35 and Or49 function null mutations. For generation of mutants and single-guide RNA (sgRNA) design, see [Figure S4A](#).

and (though weaker) Or49/Orco responded to several ITCs, with the oviposition cues iberberin, 4-pentenyl ITC, and phenylethyl ITC yielding the strongest responses ([Figures 2B–2E](#); for dose response tests, see [Figure S3](#)). Further tests with Or35/Orco and Or49/Orco with another 36 ecologically relevant

duced insertion or deletion at the site of Or35 and Or49 in G0 after injection ([Figure 3B](#)). Among diverse mutations detected from the mutated individuals, one mutation with 2-bp deletion was used to generate the Or35 homozygous knockout strain (Or35^{-/-}; [Figure 3C](#)), as this deletion introduced a stop codon

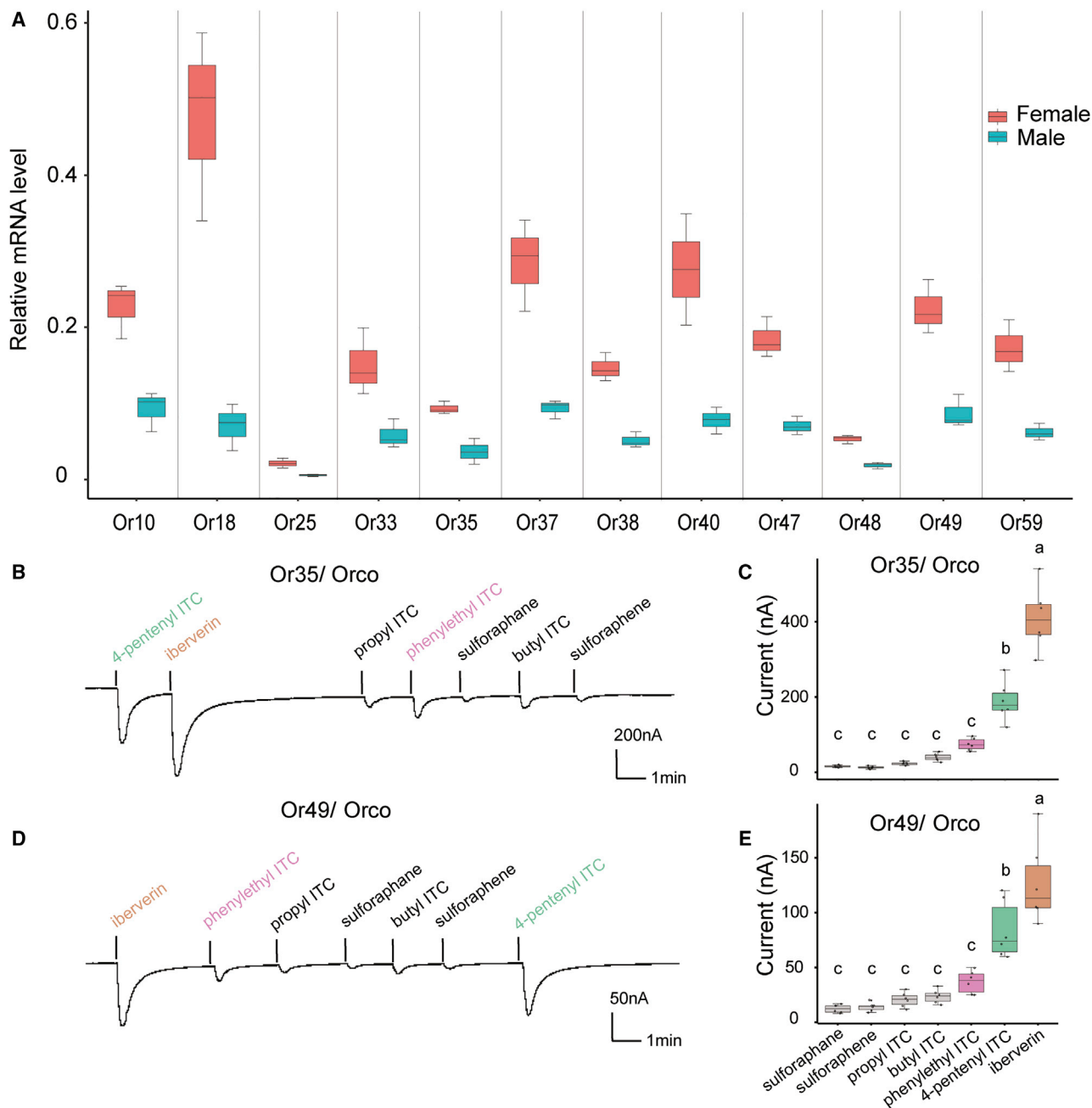


Figure 2. Female-Enhanced Receptors Or35 and Or49 Respond to Isothiocyanates

(A) qRT-PCR data from 12 Ors that exhibit at least two times higher expression in females than in males ($n = 3$).

(B) Representative two-electrode voltage-clamp traces of Or35/Orco ectopically expressed in *Xenopus* oocytes.

(C) Boxplot of current amplitudes of Or35/Orco ($n = 6$) induced by different ITCs (10^{-4} M) (one-way ANOVA followed by Tukey's pairwise test; $p < 0.05$).

(D) Representative two-electrode voltage-clamp traces of Or49/Orco ectopically expressed in *Xenopus* oocytes.

(E) Boxplot of current amplitudes of Or49/Orco ($n = 6$) induced by different ITCs (10^{-4} M) (one-way ANOVA followed by Tukey's pairwise test; $p < 0.05$).

Boxplots depict median and upper and lower quartile; whiskers depict quartiles $\pm 1.5 \times$ the interquartile range (IQR). Results of 42 other odorants that did not elicit any response during recording were not shown here. See also Figures S2 and S3 and Tables S1 and S2.

that leads to a loss-of-function protein consisting of only 109 amino acids (389 amino acids for the WT strain). For Or49, a homozygous knockout strain (*Or49*^{-/-}; Figure 3C) was generated with a 3-bp insertion and 1-bp deletion, which introduced a stop codon that lead to a loss-of-function protein consisting of

only 114 amino acids (391 amino acids for the WT strain). Finally, we also generated a homozygous *Or35/Or49* double knockout strain (*Or35*^{-/-}*Or49*^{-/-}; Figure 3C) by introducing a mutation (5-bp deletion) to *Or35* (resulting in 108 instead of 389 amino acids) in the aforementioned *Or49*^{-/-} strain. The *Or35*, *Or49*,

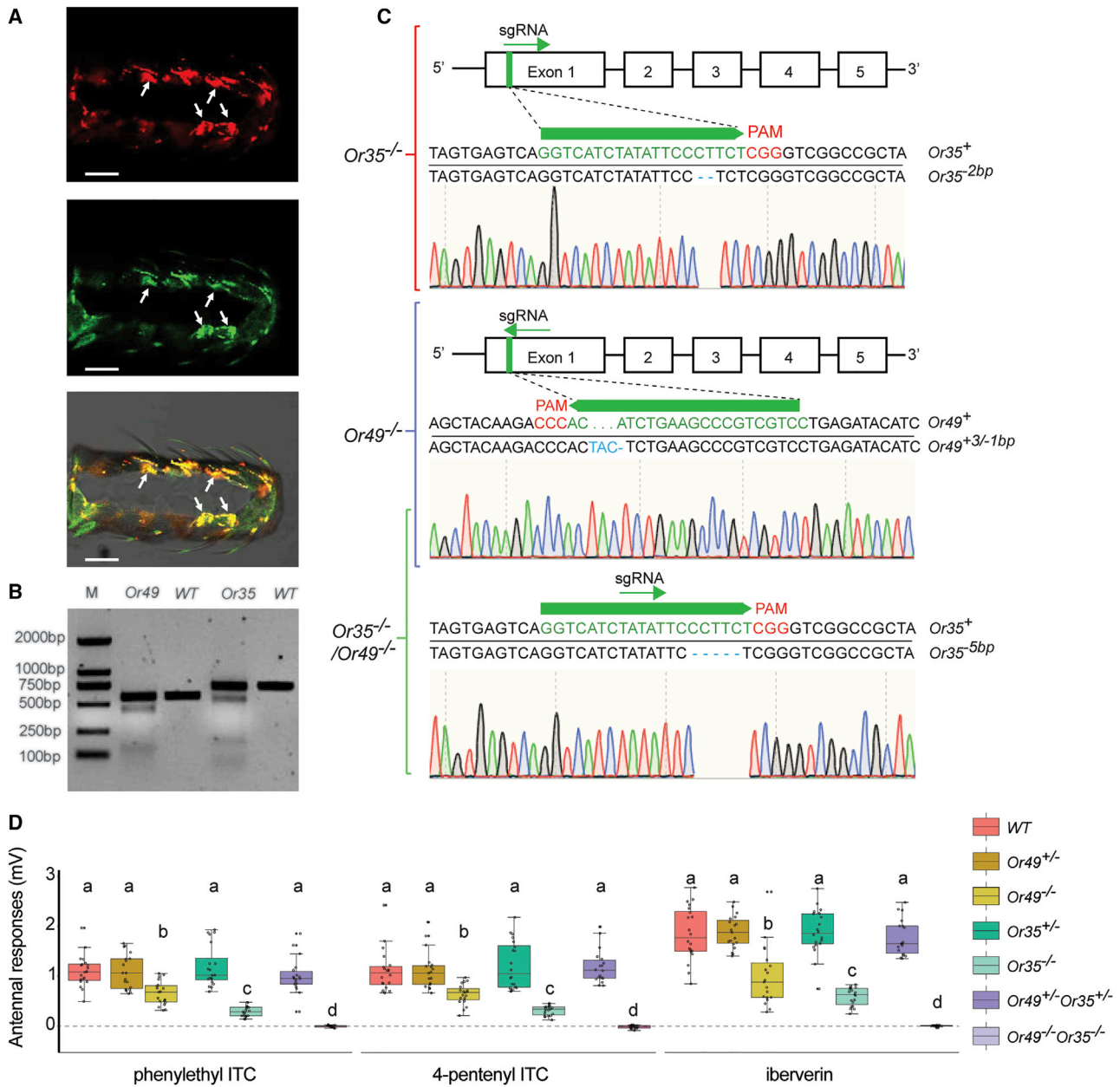


Figure 3. CRISPR-Cas9 Directed Mutagenesis of *P. xylostella* Ors

(A) *Or35* (red) and *Or49* (green) express together in trichoid sensilla as confirmed by *in situ* hybridization on cryo-section of a female antennae of *P. xylostella*. (B) Identification of CRISPR-Cas9 nickase induced indel in the *Or49* and *Or35* by T7 endonuclease 1 (T7E1) cleavage assay in the G0. Lane 1: DNA ladder; Lane 2–5: T7E1 digest of PCR product amplified from the target site of *Or49*-edited, *Or49*-unedited, *Or35*-edited, and *Or35*-unedited pools.

(C) Schematic diagram of single-guide RNA (sgRNA) targeting site of *Or35* and *Or49*. sgRNA of *Or35* and *Or49* were both designed in exon 1. sgRNA is in green. The protospacer adjacent motif (PAM) sequence is in red. The change in length is marked right of each sequence (+, insertion; –, deletion). Mutation of *Or35* with a 2-bp deletion was confirmed by sequencing (see aligned sequences). Mutation of *Or49* with a 3-bp insertion and 1-bp deletion was confirmed by sequencing (see aligned sequences). *Or35*^{-/-}*Or49*^{-/-} mutant was generated on the base of *Or49*^{-/-} mutant, which has a 5-bp deletion in *Or35*.

(D) EAG responses (the response of each animal to solvent was subtracted from the odorant responses) of *P. xylostella* female antennae (one-way ANOVA followed by Tukey's pairwise test; $p < 0.05$; $n = 18$ to 20 per genotype).

Boxplots depict median and upper and lower quartile; whiskers depict quartiles $\pm 1.5 \times$ the interquartile range (IQR). See also Figure S4 and Table S2.

and *Or35/Or49* knockout homozygous strains were obtained in three, three, and four generations, respectively.

To test the possibility of off-target effects, we amplified and sequenced the putative off-target sites and found no frameshift

or premature stop codon in any of those loci (Figures S4B and S4C). Furthermore, we found neither differences in terms of larval development and pupae weight and length, nor in emerging, mating rates, and proboscis extension response

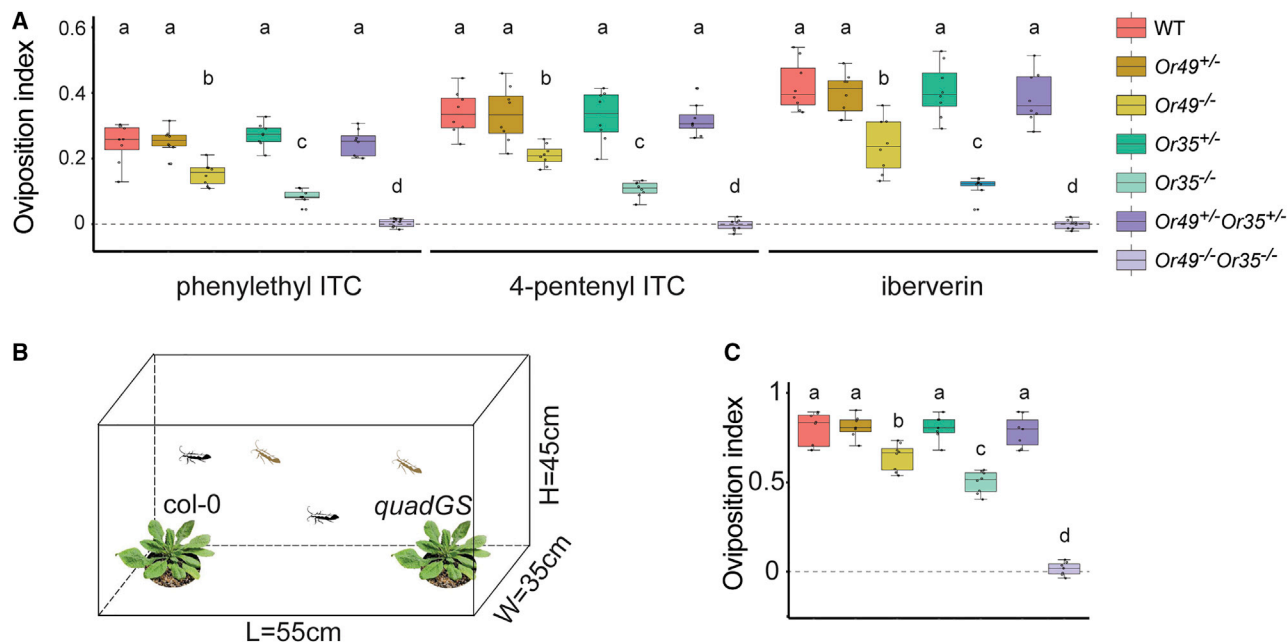


Figure 4. Or35 and Or49 Together Are Necessary and Sufficient for Detecting ITCs

(A) Oviposition index ($n = 8$) of the WT, $Or49^{+/-}$, $Or49^{-/-}$, $Or35^{+/-}$, $Or35^{-/-}$, $Or49^{+/-}Or35^{+/-}$, and $Or49^{-/-}Or35^{-/-}$ genotypes.

(B) Schematic drawing of oviposition assays with two *A. thaliana* strains.

(C) Oviposition index ($n = 7-8$) of the above-mentioned moth genotypes toward WT (*Col-0*) and GS-deficient mutant (*quadGS*) *A. thaliana*. Different letters indicate significant differences among insect genotypes (one-way ANOVA followed by Tukey's pairwise test; $p < 0.05$).

Boxplots depict median and upper and lower quartile; whiskers depict quartiles $\pm 1.5 \times$ the interquartile range (IQR). See also Figure S1 and Table S4.

(PER) (Figures S4D–S4I), suggesting that no off-target effects occurred in our study.

With the three *Or* knockout strains, we first performed EAG tests using the identified oviposition stimulants iberberin, 4-pentenyl ITC, and phenylethyl ITC. The responses to all three compounds were unaffected in the heterozygous moths ($Or35^{+/-}$, $Or49^{+/-}$, and $Or35^{+/-}Or49^{+/-}$). However, the same compounds induced only reduced responses in the homozygous females when either *Or35* or *Or49* were knocked out, and responses were completely abolished in homozygous females carrying double knockouts of *Or35* and *Or49* (Figure 3D), suggesting that both *Or35* and *Or49* are involved in ITC detection. Interestingly, $Or35^{-/-}$ moths exhibited a stronger reduction in EAG response when compared to $Or49^{-/-}$ moths, which is in accordance with higher sensitivity of *Or35* in the *Xenopus* oocyte system (Figure S3).

To confirm the behavioral roles and the relative contribution of the two *Ors*, we further conducted egg-laying tests of $Or35^{-/-}$, $Or49^{-/-}$, and $Or49^{-/-}Or35^{-/-}$ to the three ITC compounds. Consistent with the EAG results, $Or35^{-/-}$ and $Or49^{-/-}$ females showed reduced oviposition preferences to all three ITC compounds compared to WT moths, while the $Or49^{-/-}Or35^{-/-}$ females lost the oviposition preferences to the three ITC compounds completely (Figure 4A).

ITC-Deficient *A. thaliana* Plants Confirm the Necessity of Or35 and Or49 for Host Plant Choice

To investigate the necessity of *Or35* and *Or49* in ITC-based host plant choice, we tested the oviposition performance of the

different mutant moths by providing a choice of *Col-0* (WT *A. thaliana*) or *quadGS* (an ITC-deficient mutant of *A. thaliana*) (Figure 4B; Figure S1, top). While WT moths (and the different heterozygous controls) strongly preferred the ITC-emitting *A. thaliana*, this preference was significantly reduced in both single-receptor mutant moths and abolished when both *Or35* and *Or49* were knocked out (Figure 4C). Therefore, we conclude that *Or35* and *Or49* together are necessary and sufficient for host plant choice in the moth *P. xylostella*.

DISCUSSION

Many herbivorous insects seem to discriminate between host and non-host plants by detecting specific combinations of several ubiquitous aliphatics, aromatics, and terpenes, rather than taxon-specific volatiles [7, 8]. Here, however, we present evidence that a small number of host-specific compounds, i.e., the three ITCs iberberin, 4-pentenyl ITC, and phenylethyl ITC, are sufficient to govern oviposition choice of a crucifer specialist, the diamondback moth *P. xylostella*. While the ITCs' function as oviposition cues was shown before [5, 6], the mechanism of their detection in insects so far remained elusive.

To explore the mechanisms of ITC perception in the diamondback moth, we first identified and functionally characterized 12 *Ors* (from a total of 59 *Ors*) that elicited a female-biased expression, pointing at their potential involvement into oviposition behavior [9, 10]. Of these 12 *Ors*, only two, *Or35* and *Or49*, exhibited strong and specific responses to the above-mentioned ITCs when ectopically expressed in the oocyte system. The

high specificity of these two Ors supports the existence of a dedicated olfactory circuit in this crucifer specialist moth for host-specific odors, similar to the well-investigated dedicated circuits for detection of sex pheromones or compounds signifying danger [11].

Interestingly, when both receptors were knocked out, female moths lost their oviposition preference completely to the three ITC compounds and did not differentiate anymore between a WT *A. thaliana* plant and an ITC-deficient mutant of this plant. Obviously, the most important behaviorally active ITCs released by *A. thaliana* are perceived by only Or35 and Or49, and notably, these two Ors are necessary and sufficient to govern the ITC-driven moths' oviposition choice toward *A. thaliana*. As the different *A. thaliana* ecotypes have been shown to differ in their glucosinolate (GS) content (which results in different ITC breakdown products) [12], we cannot exclude that additional ITCs that were not individually tested in our study also become detected by Or35 and/or Or49 and affected the moths' choice. Furthermore, it should be mentioned that ITCs probably are not the only cues that affect the moths' oviposition choice, as moths potentially could detect non-volatile GSs via direct contact or non-ITC volatile breakdown products like nitriles [13–15]. However, as the three most active ITCs in our study have been identified not only in *A. thaliana*, but also in many cruciferous plants (Table S3), Or35 and Or49 probably generally drive the moth preference for cruciferous plants. The presence of two receptors that are both involved in the detection of the same ecologically relevant compounds could hint at the importance of this detection, as the simultaneous loss of function of two Ors by natural mutation is much lower than that of only one Or [16]. Despite their overlapping response spectra, Or35 displayed a stronger sensitivity to the ITCs than Or49. The presence of two receptors with similar tuning but different sensitivity probably allows for a precise coding of the odorant quantity over a large range of concentrations and might help the moths to target cruciferous plants from long distances. At the same time, it might facilitate the discrimination of specific plant odorant mixtures [17]. Future studies will reveal whether olfactory sensory neurons expressing Or35 and Or49 differ in number and whether different roles of both receptors can be identified by, e.g., testing the long-distance attraction of the moths.

In conclusion, the present study, for the first time, identifies the molecular basis of host selection in a cruciferous specialist. As there are more than 20 described cruciferous specialist insect species across the orders of Lepidoptera, Coleoptera, Hemiptera, and Diptera [18], it will be interesting to test whether this pathway is conserved in different species.

STAR★METHODS

Detailed methods are provided in the online version of this paper and include the following:

- KEY RESOURCES TABLE
- RESOURCE AVAILABILITY
 - Lead Contact
 - Materials Availability
 - Data and Code Availability
- EXPERIMENTAL MODEL AND SUBJECT DETAILS

- Animals and Plants
- METHOD DETAILS
 - RNA Extraction and cDNA Preparation
 - Gene Cloning and Verification of Or Genes
 - Reverse-transcriptase Quantitative PCR
 - *In Situ* Hybridization
 - *Xenopus* Oocytes System
 - *In Vitro* Synthesis of Single Guide RNA
 - Embryo Microinjection
 - Mutagenesis Detection
 - Screening Homozygote Mutants
 - Off-target Mutation Detection
 - Electroantennogram Recordings
 - Oviposition Behavioral Assays
 - Chemical Analysis

SUPPLEMENTAL INFORMATION

Supplemental Information can be found online at <https://doi.org/10.1016/j.cub.2020.08.047>.

ACKNOWLEDGMENTS

This work was supported by grants from National Natural Science Foundation, China (31672350), Sino-Euro Cooperative Project, China (2018-EU-08), and the Postgraduate Research & Practice Innovation Program of Jiangsu Province (KYCX18_0668), China. We thank Cheng-Wang Sheng and Jie Jiang for technical help with *Xenopus* system, Mei-Yan Zheng for help with embryonic injections, Si-Jie Sun and Zhi-Qiang Wei for help with insect rearing, and Long-Ji Ze and Yue Peng for help with drawing picture.

AUTHOR CONTRIBUTIONS

X.-L.L., J.Z., M.K., and S.-L.D. designed research; X.-L.L., J.Z., Q.Y., C.-L.M., W.-K.H., W.H., K.Y., Y.-C.P., and J.-M.G. performed research; X.-L.L., J.Z., S.-L.D., and M.K. analyzed data; and X.-L.L., J.Z., Q.Y., B.S.H., H.X., C.-Z.W., S.-L.D., and M.K. wrote the paper.

DECLARATION OF INTERESTS

The authors declare no competing interests.

Received: March 23, 2020

Revised: June 22, 2020

Accepted: August 12, 2020

Published: September 10, 2020

REFERENCES

1. Fahey, J.W., Zalcman, A.T., and Talalay, P. (2001). The chemical diversity and distribution of glucosinolates and isothiocyanates among plants. *Phytochemistry* 56, 5–51.
2. Halkier, B.A., and Gershenzon, J. (2006). Biology and biochemistry of glucosinolates. *Annu. Rev. Plant Biol.* 57, 303–333.
3. Cartea, M.E., and Velasco, P. (2008). Glucosinolates in Brassica foods: bioavailability in food and significance for human health. *Phytochem. Rev.* 7, 213–229.
4. Städler, E., and Reifennath, K. (2009). Glucosinolates on the leaf surface perceived by insect herbivores: review of ambiguous results and new investigations. *Phytochem. Rev.* 8, 207–225.
5. Sun, J.Y., Sønderby, I.E., Halkier, B.A., Jander, G., and de Vos, M. (2009). Non-volatile intact indole glucosinolates are host recognition cues for ovipositing *Plutella xylostella*. *J. Chem. Ecol.* 35, 1427–1436.

6. Renwick, J.A.A., Haribal, M., Gouinguéné, S., and Städler, E. (2006). Isothiocyanates stimulating oviposition by the diamondback moth, *Plutella xylostella*. *J. Chem. Ecol.* **32**, 755–766.
7. Bruce, T.J.A., Wadhams, L.J., and Woodcock, C.M. (2005). Insect host location: a volatile situation. *Trends Plant Sci.* **10**, 269–274.
8. Bruce, T.J.A., and Pickett, J.A. (2011). Perception of plant volatile blends by herbivorous insects—finding the right mix. *Phytochemistry* **72**, 1605–1611.
9. Liu, C., Liu, Y., Guo, M., Cao, D., Dong, S., and Wang, G. (2014). Narrow tuning of an odorant receptor to plant volatiles in *Spodoptera exigua* (Hübner). *Insect Mol. Biol.* **23**, 487–496.
10. Wu, H., Li, R.T., Dong, J.F., Jiang, N.J., Huang, L.Q., and Wang, C.Z. (2019). An odorant receptor and glomerulus responding to farnesene in *Helicoverpa assulta* (Lepidoptera: Noctuidae). *Insect Biochem. Mol. Biol.* **115**, 103106.
11. Haverkamp, A., Hansson, B.S., and Knaden, M. (2018). Combinatorial codes and labeled lines: How insects use olfactory cues to find and judge food, mates, and oviposition sites in complex environments. *Front. Physiol.* **9**, 49.
12. Brown, P.D., Tokuhisa, J.G., Reichelt, M., and Gershenzon, J. (2003). Variation of glucosinolate accumulation among different organs and developmental stages of *Arabidopsis thaliana*. *Phytochemistry* **62**, 471–481.
13. Jeschke, V., Kearney, E.E., Schramm, K., Kunert, G., Shekhov, A., Gershenzon, J., and Vassão, D.G. (2017). How glucosinolates affect generalist Lepidopteran larvae: Growth, development and glucosinolate metabolism. *Front. Plant Sci.* **8**, 1995.
14. Lambrix, V., Reichelt, M., Mitchell-Olds, T., Kliebenstein, D.J., and Gershenzon, J. (2001). The *Arabidopsis* epithiospecifier protein promotes the hydrolysis of glucosinolates to nitriles and influences *Trichoplusia ni* herbivory. *Plant Cell* **13**, 2793–2807.
15. Burow, M., Losansky, A., Müller, R., Plock, A., Kliebenstein, D.J., and Wittstock, U. (2009). The genetic basis of constitutive and herbivore-induced ESP-independent nitrile formation in *Arabidopsis*. *Plant Physiol.* **149**, 561–574.
16. Andersson, M.N., Löfstedt, C., and Newcomb, R.D. (2015). Insect olfaction and the evolution of receptor tuning. *Front. Ecol. Evol.* **3**, 1–13.
17. de Fouchier, A., Walker, W.B., 3rd, Montagné, N., Steiner, C., Binyameen, M., Schlyter, F., Chertemps, T., Maria, A., François, M.C., Monsempe, C., et al. (2017). Functional evolution of Lepidoptera olfactory receptors revealed by deorphanization of a moth repertoire. *Nat. Commun.* **8**, 15709.
18. Hopkins, R.J., van Dam, N.M., and van Loon, J.J.A. (2009). Role of glucosinolates in insect-plant relationships and multitrophic interactions. *Annu. Rev. Entomol.* **54**, 57–83.
19. Müller, R., de Vos, M., Sun, J.Y., Sønderby, I.E., Halkier, B.A., Wittstock, U., and Jander, G. (2010). Differential effects of indole and aliphatic glucosinolates on lepidopteran herbivores. *J. Chem. Ecol.* **36**, 905–913.
20. Li, X., Liu, J., Gong, L., Chen, Y., and Zhong, G. (2011). Cloning and expression of odorant receptor gene PxyOr83b from *Plutella xylostella* (Lepidoptera: Plutellidae). *Acta Entomologica Sinica* **54**, 502–507.
21. Sun, M., Liu, Y., Walker, W.B., Liu, C., Lin, K., Gu, S., Zhang, Y., Zhou, J., and Wang, G. (2013). Identification and characterization of pheromone receptors and interplay between receptors and pheromone binding proteins in the diamondback moth, *Plutella xylostella*. *PLoS ONE* **8**, e62098.
22. Kong, C., Wang, G., Liu, Y., and Yan, S. (2014). Gene cloning and expression analysis of three odorant receptors in the diamondback moth (*Plutella xylostella*). *Scientia Agricultura Sinica* **47**, 1735–1742.
23. Liu, Y., Liu, Y., Yang, T., Gui, F., and Wang, G. (2015). Identification and characterization of a general odorant receptor gene PxyOr9 in the diamondback moth, *Plutella xylostella* (Lepidoptera: Plutellidae). *Acta Entomologica Sinica* **58**, 507–515.
24. Liu, Y., Liu, Y., Jiang, X., and Wang, G. (2018). Cloning and functional characterization of three new pheromone receptors from the diamondback moth, *Plutella xylostella*. *J. Insect Physiol.* **107**, 14–22.
25. You, M., Yue, Z., He, W., Yang, X., Yang, G., Xie, M., Zhan, D., Baxter, S.W., Vasseur, L., Gurr, G.M., et al. (2013). A heterozygous moth genome provides insights into herbivory and detoxification. *Nat. Genet.* **45**, 220–225.
26. Engsontia, P., Sangket, U., Chotigeat, W., and Satasook, C. (2014). Molecular evolution of the odorant and gustatory receptor genes in lepidopteran insects: implications for their adaptation and speciation. *J. Mol. Evol.* **79**, 21–39.
27. Krieger, J., Raming, K., Dewey, Y.M., Bette, S., Conzelmann, S., and Breer, H. (2002). A divergent gene family encoding candidate olfactory receptors of the moth *Heliothis virescens*. *Eur. J. Neurosci.* **16**, 619–628.
28. Yang, K., Huang, L.Q., Ning, C., and Wang, C.Z. (2017). Two single-point mutations shift the ligand selectivity of a pheromone receptor between two closely related moth species. *eLife* **6**, e29100.
29. Liu, X.L., Sun, S.J., Khuhro, S.A., Elzaki, M.E.A., Yan, Q., and Dong, S.L. (2019). Functional characterization of pheromone receptors in the moth *Aethes dissimilis* (Lepidoptera: Noctuidae). *Pestic. Biochem. Physiol.* **158**, 69–76.
30. Xiao, A., Cheng, Z., Kong, L., Zhu, Z., Lin, S., Gao, G., and Zhang, B. (2014). CasOT: a genome-wide Cas9/gRNA off-target searching tool. *Bioinformatics* **30**, 1180–1182.
31. Yang, M., Dong, S., and Chen, L. (2009). Electrophysiological and Behavioral Responses of Female Beet Armyworm *Spodoptera exigua* (Hübner) to the Conspecific Female Sex Pheromone. *J. Insect Behav.* **22**, 153–164.
32. Xu, Z., Cao, G.C., and Dong, S.L. (2010). Changes of sex pheromone communication systems associated with tebufenozide and abamectin resistance in diamondback moth, *Plutella xylostella* (L.). *J. Chem. Ecol.* **36**, 526–534.
33. Rohloff, J., and Bones, A.M. (2005). Volatile profiling of *Arabidopsis thaliana* - putative olfactory compounds in plant communication. *Phytochemistry* **66**, 1941–1955.

STAR★METHODS

KEY RESOURCES TABLE

REAGENT or RESOURCE	SOURCE	IDENTIFIER
Isothiocyanates		
Methyl ITC	TCI Shanghai	I0189
Ethyl ITC	TCI Shanghai	I0188
Propyl ITC	TCI Shanghai	I0388
Butyl ITC	TCI Shanghai	I0249
Allyl ITC	Sigma-Aldrich	36682
4-Pentenyl ITC	TCI Shanghai	I0444
Phenyl ITC	TCI Shanghai	I0191
Benzyl ITC	TCI Shanghai	I0224
Phenylethyl ITC	TCI Shanghai	P0986
4-Methoxyphenyl ITC	TCI Shanghai	I0513
Iberverin	TCI Shanghai	M2027
Sulforaphane	Greenpure Chengdu	BP0219
Sulforaphene	Greenpure Chengdu	BP0218
Sex pheromones and analogs		
(Z)-11-hexadecenal	Nimord Changzhou	53939-28-9
(Z)-11-hexadecenyl acetate	Nimord Changzhou	34010-21-4
(Z)-11-hexadeceno	Nimord Changzhou	56683-54-6
(Z)-9-tetradecenyl acetate	Nimord Changzhou	16725-53-4
(Z)-9-tetradecenyl alcohol	Nimord Changzhou	35153-15-2
(Z)-9-hexadecen-1-yl acetate	Nimord Changzhou	34010-20-3
(Z,E)-9,12-tetradecadienol	Nimord Changzhou	42521-46-0
(Z)-9-hexadecenal	Nimord Changzhou	56219-04-6
(Z)-9-tetradecenal	Nimord Changzhou	53939-27-8
(Z)-9-Hexadecenol	Nimord Changzhou	10378-01-5
(Z,E)-9,12-tetradecadienyl acetate	Nimord Changzhou	31654-77-0
Plant odorants		
(z)-3-hexen-1-o	Sigma-Aldrich	W256307
(E)-2-hexanal	TCI Shanghai	H0345
Hexanal	TCI Shanghai	H0133
Hexanol	Sigma-Aldrich	471402
Heptaldehyde	Sigma-Aldrich	W254002
Ocimene	meryer	M06010
(Z)-3-hexenol acetate	TCI Shanghai	A0888
(E)-2-Hexen-1-ol	TCI Shanghai	H0346
1-Nonanol	Aladdin	N105714
Myrcene	Sigma-Aldrich	64643
α -Pinene	TCI Shanghai	P1099
Linalool	TCI Shanghai	L0048
Geraniol	Sigma-Aldrich	163333
β -caryophyllen	Sigma-Aldrich	22075
1,8-Cineole	Sigma-Aldrich	C80601
Benzaldehyde	Sigma-Aldrich	418099
α -Farnesene	Sigma-Aldrich	W383902
Nonane	TCI Shanghai	N0286

(Continued on next page)

Continued

REAGENT or RESOURCE	SOURCE	IDENTIFIER
Decane	TCI Shanghai	D0011
1-Nonanal	TCI Shanghai	N0296
Benzoic acid	TCI Shanghai	B2635
(E)-3-Hexen-1-ol	Sigma-Aldrich	224715
Camphene	TCI Shanghai	L0046
α -Terpinene	Sigma-Aldrich	456055
Limonene	Sigma-Aldrich	86473
Others		
pEASY-Blunt3 cloning kit	TransGenBiotech Beijing	CB301-02
ChamQ Universal SYBR qPCR Master Mix	Vazyme Nanjing	Q711-03
HiScript® III SuperMix for qPCR kit	Vazyme Nanjing	R323-01
Mix Precision gRNA Synthesis Kit	Ambion	A29377
Software and Algorithms		
Prism 7.04	GraphPad	https://www.graphpad.com/scientific-software/prism/
SPSS 17.0	IBM	https://spss.en.softonic.com/
ORFfinder	NCBI	https://www.ncbi.nlm.nih.gov/orffinder/
TMHMM Server Version 2.0	N/A	http://www.cbs.dtu.dk/services/TMHMM

RESOURCE AVAILABILITY**Lead Contact**

Further information and requests for resources should be directed to and will be fulfilled by the Lead Contact, Shuang-Lin Dong (sldong@njau.edu.cn).

Materials Availability

This study did not generate new unique reagents.

Data and Code Availability

The datasets of accession numbers for Ors and primers used during this study are available as [Supplemental Information](#).

EXPERIMENTAL MODEL AND SUBJECT DETAILS**Animals and Plants**

Plutella xylostella larvae were reared on the radish (*Raphanus sativus* L.) seedlings at $27 \pm 1^\circ\text{C}$ with 16 L: 8 D photoperiod and 65 ± 5 RH% in an insect rearing room. Male and female pupae were separated and maintained in cages until eclosion. The adults were supplied with 10% honey solution.

Wild type (Col-0) and mutant (*quadGS*) *Arabidopsis thaliana* plant seeds were kindly provided by Prof. Philippe Reymond from University of Lausanne, Lausanne, Switzerland [19]. The plants were cultured in a climate chamber ($23 \pm 1^\circ\text{C}$, 16 L: 8 D and 65 ± 5 RH%). Plants were allowed to grow for three to four weeks (before flowering) before the tests. Plants were transferred to the insect rearing room for 3 days before the experiment.

Female *Xenopus laevis* were group housed in the recirculating aquaculture system with purified water in $22 \pm 1^\circ\text{C}$, and reared with beef liver in the rearing room. The use of *X. laevis* strictly followed the Nanjing Agricultural University guidelines for animal protection and welfare.

METHOD DETAILS**RNA Extraction and cDNA Preparation**

A mix of virgin male and female antennae was collected for gene cloning. To determine the transcript level of target gene in different adult tissues, the antennae, heads, legs and wings were collected from virgin male and female adults, respectively. The collected tissues were frozen in liquid nitrogen and stored at -80°C until use for RNA extraction. Total RNA was extracted by Trizol Reagent (Invitrogen, Carlsbad, USA) following the manufacturer's protocol. The first single strand cDNAs were synthesized using HiScript® III RT SuperMix for qPCR kit (+gDNA wiper) (Vazyme, Nanjing, China).

Gene Cloning and Verification of Or Genes

Li et al. (2011) [20] reported the full length *Orco* cDNA. Sun et al. (2013) [21], Sun et al. (2014) [22], Liu et al. (2015, 2018) [23, 24] cloned and functionally identified 13 Ors (*Or1, 3, 4, 5, 6, 7, 8, 9, 16, 17, 18, 41* and *45*) in *P. xylostella*. In addition, You et al. (2013) [25] reported *P. xylostella* genome sequence and annotated 79 Or genes by analysis of the genome sequence, and Engsontia et al. (2014) [26] reported 95 Or genes by re-analyzing the same genome sequence data, but these Ors were not verified. Furthermore, we conducted a transcriptome analysis of adult antennae and identified 6 new candidate Or genes (GenBank accession numbers: MT_418911-MT_418916). To verify these reported Ors, we first aligned and compared all Ors' amino acid sequences using ClustalW to remove the repetitive sequences, and obtained 63 full length and 6 partial length Ors. Then we carried out end-to-end PCR to verify the full-length sequences of those 63 full length Ors. The PCR reaction mixture containing 12.5 μ L of 2 \times Phanta Max Master Mix, 9.5 μ L of ddH₂O, 1 μ L of cDNA template and 1 μ L of each primer (10 μ M). The PCR program was set at 95°C for 3 min, 34 cycles of 95°C for 15 s, 55°C for 15 s, 72°C for 1 min 30 s, and 72°C for 5 min. PCR products were analyzed by electrophoresis on a 1.2% agarose gel. Target bands were purified and cloned into a pEASY-Blunt3 cloning vector (TransGen Biotech, Beijing, China) and sequenced at GenScript Company (Nanjing, China). The full-length open-reading frames (ORF) of these genes were predicted using the ORFfinder. Transmembrane domains of amino-acid sequences were predicted by TMHMM Server Version 2.0. We successfully verified 59 Or genes, including the *Orco* (Li et al., 2011) [20], the 13 Ors by Sun et al. (2013) [21], Sun et al. (2014) [22] and Liu et al. (2015, 2018) [23, 24], 39 Ors by You et al. (2013) [25] and Engsontia et al. (2014) [26], and 6 Ors (the GenBank accession number of *Or49, 33, 47, 50, 54* and *58*: MT418911- MT418916) from our transcriptome data.

Reverse-transcriptase Quantitative PCR

To compare the transcription levels of each Or between male and female antennae, qRT-PCR was conducted. Among the 59 verified Ors, 9 Ors (*Or1, 3, 4, 5, 6, 7, 8, 41* and *45*) had been reported with this regard by Sun et al. (2013) [21] and Liu et al. (2015, 2018) [23, 24], therefore the other 50 Ors were measured in the present study. The specific primers used for quantification of target genes were designed by Beacon Designer 8.0 (PRIMER Biosoft International, CA, USA) (Table S1). qRT-PCR was performed on a QuantStudio 6 Flex Real-Time PCR System (Applied Biosystems, Foster City, CA, USA) with ChamQTM Universal SYBR[®] qPCR Master Mix (Vazyme, Nanjing, China). qRT-PCR reaction mixture contained 10 μ L of 2 \times ChamQ Universal SYBR qPCR Master Mix, 0.4 μ L of each of forward and reverse gene-specific primer, 1 μ L of cDNA template, and 8.2 μ L of nuclease-free water to a final volume of 20 μ L. qRT-PCR cycling parameters were set at 95°C for 30 s, 40 cycles of 95°C for 5 s and 60°C for 34 s. The glyceraldehyde-3-phosphate dehydrogenase (*GAPDH*) and ribosomal protein S3 (*RPS3*) were used as two reference genes to calculate Δ Ct following the formula: Δ Ct = Ct of target gene – avg. Ct of two reference genes. Target gene expression levels were analyzed using the 2^{− Δ CT} method. For each gene, three independent biological replicates were measured.

In Situ Hybridization

Two-color double *in situ* hybridizations were performed following protocols reported previously [27, 28]. Briefly, the primers were used to synthesize the gene-specific probes from the open-reading frames. For *PxylOr35*, Forward: CGAGCAATTAAGACGATCG TAAGCAG; Reverse: GATATAAAAAGTGGCCACCGTCACATC; For *PxylOr49*, Forward: GCTATCGGACTTGGAGAGAACTCAGC; Reverse: GAATATGAGTACACTGTTGGTGGTGGC. Both digoxin (Dig)-labeled and biotin (Bio)-labeled probes were synthesized by DIG RNA labeling Kit version 12 (SP6/T7) (Roche, Mannheim, Germany), with Dig-NTP or Bio-NTP (Roche, Mannheim, Germany) labeling mixture, respectively. RNA probes were subsequently fragmented to 300 nt by incubation in carbonate buffer. Antennae were dissected from 3- to 5-day-old wild-type female moths, embedded in JUNG tissue freezing medium (Leica, Nussloch, Germany) and sections (12 μ m) were prepared with a Leica CM1950 microtome at −22°C, then mounted on Super Frost Plus slides (Thermo Scientific, Waltham, MA). After a series of fixing and washing procedures, 100 mL hybridization solution (Boster, Wuhan, China) containing both Dig and Bio probes was placed onto the tissue sections and incubated at 55°C overnight. After hybridization, slides were washed and incubated for 60 min with anti-digoxigen (Roche, Mannheim, Germany) and Streptavidin-HRP (PerkinElmer, Boston, MA). Hybridization signals were visualized by incubating the sections for 40 min with HNPP/Fast Red (Roche, Mannheim, Germany) and Biotinyl Tyramide Working Solution for 10 min at room temperature followed by the tyramide-signal amplification (TSA) kit protocols (PerkinElmer, Boston, MA). All the sections were analyzed under a Zeiss LSM710 Meta laser scanning microscope (Zeiss, Oberkochen, Germany).

Xenopus Oocytes System

Vector construction, cRNA synthesis and electrophysiological recording by *Xenopus* oocytes system were performed using the methods described previously [29].

In Vitro Synthesis of Single Guide RNA

According to the principle of 5 \prime -CCNN 18 CC-3 \prime , the sgRNA target sites of both *Or35* and *Or49* were designed on exon 1. No potential off-target sites were found at other gene regions, during the design of sgRNA. The sgRNAs were synthesized with Precision gRNA Synthesis Kit (Ambion, Foster City, CA), and purified with gRNA Clean Up Kit (Ambion, Foster City, CA) according to the manufacturer's instruction. The transcribed sgRNAs were quantified using a NanoDrop ND-1000 spectrophotometer (Thermo Fisher Scientific, Waltham, MA, USA), and then diluted to 700 ng/ μ L in RNase-free water and stored at −80°C.

Embryo Microinjection

The parafilm was painted with radish seedlings juice to stimulate the oviposition behavior of female adults. The parafilm was checked at intervals of 30 min to collect fresh eggs. The eggs were lined up on a microscope slide (fixed with double-sided adhesive tape). The mixture composed of sgRNA (350 ng/ μ L) and Cas9 protein (200 ng/ μ L) (Thermo Fisher Scientific, Shanghai, China) was injected into individual eggs within 2 h after oviposition using a FemtoJet and InjectMan NI 2 microinjection system (Eppendorf, Hamburg, Germany). The injected eggs were returned to normal rearing conditions for hatching. Flour on the slide ensured larval survival on the double-sided adhesive tape.

Mutagenesis Detection

To detect possible mutations, around 20 injected eggs were collected 24 h after injection. The genomic DNA was extracted from these eggs using a QIAamp DNA Mini Kit (QIAGEN, Hilden, Germany). Extracted genomic DNA was used as a template and a pair of gene-specific primer (Table S2) flanking the sgRNA targeted site was used to amplify the target DNA sequences by PCR procedures. The PCR mixture (in a total volume of 25 μ L) contained 12.5 μ L of 2 \times Rapid Taq Master Mix, 9.5 μ L of ddH₂O, 1 μ L of cDNA template and 1 μ L of each forward and reverse primer (10 μ M). The PCR program was set at 95°C for 3 min, 34 cycles of 95°C for 15 s, 55°C for 15 s, 72°C for 15 s, and 72°C for 5 min. PCR products were directly sequenced by the company. At the same time, amplified PCR products were run on a 1.2% agarose gel and target bands were purified using AxyPrep PCP Cleanup Kit (Axygen, Suzhou, Jiangsu, China). The recovered PCR products were digested with the T7EI enzyme (New England Biolabs, Ipswich, MA, USA), and occurrence of additional band on the gel electrophoresis demonstrated mutations occurred.

Screening Homozygote Mutants

G0 adults were randomly mated in single pairs, and each pair of adults was allowed to mate and lay eggs in a plastic cup. After oviposition, the genomic DNA of individual adults was extracted using DNAiso Reagent (TaKaRa, Dalian, Liaoning, China). The genotypes of G0 adults were verified by direct sequencing. A cluster of multiple sequencing peaks occurred near the sgRNA target site of Cas9 and represented a chimeric mutation in G0 adults. To investigate the InDel sequences induced by non-homologous end joining (NHEJ), PCR products were further cloned into the pEASY-T3 vector and positive clones were selected for sequencing.

The progeny of chimeric mutant G0 adults were raised as G1 larvae, and G1 adults were randomly mated in single pairs. After oviposition, the mutation genotypes of each G1 moths were checked by direct sequencing as described in G0 adults. The progeny of G1 adults with mutation genotypes that introduce a terminator codon resulting in loss-of-function protein was raised as G2 larvae. The G2 adults were randomly mated in single pairs, and after oviposition, the mutation genotype was checked as above to screen for homozygotes. The heterozygous strains used in this study were generated by crossing homozygous mutant strain with WT, and the genotype of heterozygotes was confirmed by sequencing.

Off-target Mutation Detection

Off-target effects usually occur with non-target genomic loci (fragments) that share high similarity with the seed region (12 nt) of sgRNA. The CasOT tool [30] was used to search the genome database for the potential off-target loci, and the top 5 potential off-target loci were checked for possible off-target mutations. The fragments including the potential off-target sites were PCR amplified and sequenced.

To compare biological parameters among four insect strains, 30 newly hatched larvae from each strain were randomly selected and reared for observation. The size and weight of the 2 day-old pupae were recorded. The 10 newly emerged female adults were starved for 12 h and then were tested for proboscis extension reflex (PER). The 10 pairs of 2 day-old females and males were used for mating experiments in a box (same dimension as oviposition box); mating pairs were recorded for each half h, and total pairs of mating were calculated in 3 h.

Electroantennogram Recordings

We first measured the EAG response of female antennae to 10 μ L *A. thaliana* leaf homogenate (water as solvent) and 10 μ L water (negative control). Next, we tested the EAG response to the 13 isothiocyanates components (hexane/ methanol as solvent) and solvent was used as the control. The response to solvent was subtracted. EAG values were recorded according to the standard method [31, 32]. Briefly, antennae of virgin female adults (2 days after eclosion) were cut off at the base of head with a knife and several terminal segments of the antenna were excised in order to keep better contact. The antenna was connected by gel (SPECTRA 360, Fairfield, NJ, USA) to the two recording electrodes, respectively. The filter paper strip (2.5 \times 0.75 cm) containing 1 μ g test solution or control solution was allowed to evaporate solvent for 3 min, then the paper strip was inserted into a Pasteur pipette.

The base of the pipette was connected to rubber tube and the tip of the pipette was inserted into the hole on the main airflow metal tube in which a continuous flow keep 4 mL/s was blown onto the prepared antenna. Using a stimulus controller, we generated a pulse flow (4 mL/s) through the large end of the Pasteur pipette, transporting the volatiles to the antenna for stimulation with 0.5 s pulse duration. Each component was tested twice and at least 30 s was allowed between two stimuli for recovery of antennal responsiveness. The amplitude of the EAG response was recorded and digitized with EAG-adapted software (Syntech®, the Netherlands). EAG amplitudes were calculated by subtracting the solvent response.

Oviposition Behavioral Assays

We measured the oviposition preference of wildtype *P. xylostella* to the *A. thaliana* leaf homogenate by using a two-choice assay in a cage (55 × 35 × 45 cm). Eight replicates were conducted. Briefly, we put 0.5g homogenate in 0.5 mL water and water alone on a filter disc (7-cm-diameter) in a 9-cm-diameter Petri dish; each Petri dish was covered with parafilm to which 16 holes was pricked using a pin to make odorants evaporate slowly. Treatment and control Petri dishes were placed at the opposite zones of the cage. A small plastic cup filled with 10% sugar solution was placed in the middle of the cage. Then, 10 pairs of female and male moths were released into each cage right before the scotophase started, and the number of eggs on each parafilm that covered the Petri dish was counted 24 h later. The Oviposition preference indices were calculated as $(T-C) / (T+C)$, where T is the number of eggs on the treatment side and C is the number of eggs on the control side.

For the ITC treatments, we put odorants (15 μg ITC) or solvent (hexane or methanol) on a filter disc and conducted the test according to the method as above-mentioned. To test the response of *Or35*, *Or49* and *Or35Or49* knockout strains to different *A. thaliana* lines, we put *A. thaliana* wild-type (*Col-0*) and mutated *A. thaliana* (*quadGS*, which is nearly devoid of major classes of foliar GSs) at the opposite zones in each cage. Again, females were allowed to oviposit for 24 h. We then counted the eggs that were oviposited on the different plants and calculated the oviposition index accordingly.

Chemical Analysis

To verify that GS-deficient *A. thaliana* plant no longer released the 3 behaviorally active ITCs (iberverin, 4-pentenyl ITC and phenylethyl ITC), volatiles of GS-deficient *A. thaliana* (before flowering) were identified using SPME coupled with GC/MS, with the wild-type *A. thaliana* (before flowering) plant as the control. The analysis by SPME coupled with GC/MS was conducted as previously described [33].